Engineering Conferences International
ECI Digital Archives

5th International Conference on Porous Media and Their Applications in Science, Engineering and Industry

Refereed Proceedings

Summer 6-26-2014

Keynote Talk – Novel convective heat transfer enhancement in channels and tubes filled with nanofluid-saturated metal foams

Fumika Sakai
Nonnovative Design & Technology

Wenhao Li
Graduate School of Shizuoka University

Akira Nakayama
Graduate School of Shizuoka University

Proceedings of the 5th International Conference on Porous Media and its Applications in Science and Engineering
ICPM5
June 22-27, 2014, Kona, Hawaii

NOVEL CONVECTIVE HEAT TRANSFER ENHANCEMENT IN CHANNELS AND TUBES FILLED WITH NANOFLUID

Fumika Sakai
Nonnovative Design & Technology, 1-4-10-7 Shin-Miyakoda, Kita-ku, Hamamatsu, 431-2103 Japan

Wenhao Li and Akira Nakayama
Graduate School of Shizuoka University, 3-5-1 Johoku, Naka-ku, Hamamatsu 432-8561, Japan

ABSTRACT
A local thermal non-equilibrium theory was exploited to investigate heat transfer in nanofluid saturated porous media, in view of possible heat transfer applications of metal foams filled with nanofluids as high performance heat exchangers. The resulting set of the macroscopic equations based on the modified Buongiorno model proposed by Yan et al. for convective heat transfer in nanofluids were used to obtain the analytical solutions for laminar fully developed forced convection in channels and tubes filled with nanofluid saturated metal foams. The analytical and numerical solutions were obtained for laminar fully developed forced convection in channels and tubes filled with nanofluid saturated metal foams. These solutions reveal that combination of the metal foams and nanofluids is quite effective to attain unconventionally high heat transfer performance, namely, 80 to 100 times more than the case of base fluid convection without a metal foam and thus can be used for next generation high performance heat exchangers.

INTRODUCTION
Metal foams such as aluminum material have high permeability, specific surface and thermal conductivity. Thus, they are considered to be possible candidates for compact heat exchangers, not only because of their high specific surface and thermal conductivity, but also because of thermal dispersion resulting from porous matrices. Nanofluids, on the other hand, have been focussed extensively for these years, in view of their great potential as a high-energy carrier due to their promising feature of high effective thermal conductivity. Hence, the combination of the metal foams and nanofluids, namely, nanofluid saturated metal foams may lead us to high performance heat exchangers which guarantee novel convective heat transfer enhancement.

Yang et al. [1, 2] obtained a series of exact solutions for laminar fully developed forced convection in channels and tubes, solving the two-component four-equation nonhomogeneous equilibrium model for mass, momentum and heat transfer in nanofluids, derived by Buongiorno [3]. They theoretically confirmed the possibility of anomalous convective heat transfer enhancement associated with nanofluids, in which the resulting heat transfer coefficient exceeds the level expected from the increase in the effective thermal properties of nanofluids.

Theoretical analyses on convective flows in porous media filled with nanofluids are scarce and limited to convective flows with constant diffusion coefficients, e.g. [4, 5]. Neither temperature dependence of the Brownian diffusion coefficient nor nanoparticle volume fraction dependence of the thermophoretic diffusion coefficient is considered in these previous investigations. Furthermore, neither dispersion nor tortuosity in porous media is taken into full consideration. Sakai et al. [6] recently provided a local thermal equilibrium analysis which takes account of all these effects on heat transfer, such as particle loading dependency, temperature dependency, dispersion and tortuosity in nanofluid saturated porous media along with nanofluid density variation, for the first time. Analytical solutions are obtained for laminar fully developed forced convection in channels and tubes filled with nanofluid saturated metal foams. However, as pointed out in [1, 2], the assumption of local thermal equilibrium may fail in the cases in which the solid thermal conductivity is much higher than that of the saturated fluid, such as in the case of aluminum-water combination. In this study, we shall carry out two-energy equation approach based on local thermal non-equilibrium using the modified Buongiorno model [1] so as to investigate the novel heat transfer enhancement associated with nanofluid saturated metal foams.

CONSERVATION EQUATIONS FOR NANOFLUIDS
Yang et al. [1] modified Buongiorno model [3], which assumes incompressible flow, no chemical reactions, negligible external forces, dilute mixture, negligible viscous dissipation, negligible radiative heat transfer, and local thermal equilibrium between nanoparticles and

base fluid. This modified two-component mixture model which allows the nanofluid density variation in mass, momentum and energy conservations are given, for the case of the steady flow, by

$$\frac{\partial \rho_f u_j}{\partial x_j} = 0 \tag{1}$$

$$\rho_f u_j \frac{\partial u_j}{\partial x_j} = -\frac{\partial p}{\partial x_i} + \frac{\partial}{\partial x_j}\mu_f\left(\frac{\partial u_i}{\partial x_j} + \frac{\partial u_j}{\partial x_i}\right) \tag{2}$$

$$\rho_f c_f u_j \frac{\partial T}{\partial x_j} = \frac{\partial}{\partial x_j} k_f \frac{\partial T}{\partial x_j} \tag{3}$$

$$\rho_p \frac{\partial u_j \phi}{\partial x_j} = \frac{\partial}{\partial x_j}\left(\rho_p D_B \frac{\partial \phi}{\partial x_j} + \frac{\rho_p D_T}{T}\frac{\partial T}{\partial x_j}\right) \tag{4}$$

where ρ_f, c_f, μ_f and k_f are the density, heat capacity, viscosity and thermal conductivity of the nanofluid, which depend on the nanoparticle volume fraction ϕ as ,

$$\rho_f = \phi\rho_p + (1-\phi)\rho_{bf} \tag{5a}$$

$$c_f = \left(\phi\rho_p c_p + (1-\phi)\rho_{bf} c_{bf}\right)/\rho \tag{5b}$$

$$\mu_f = \mu_{bf}\left(1 + a_\mu\phi + b_\mu\phi^2\right) = \mu_{bf}\left(1 + 7.3\phi + 123\phi^2\right) \tag{5c}$$

$$k_f = k_{bf}\left(1 + a_k\phi + b_k\phi^2\right) = k_{bf}\left(1 + 2.72\phi + 4.97\phi^2\right) \tag{5d}$$

The Brownian and thermophoretic diffusion coefficients are given by

$$D_B = k_{BO}T/3\pi\mu_{bf}d_p \tag{6a}$$

and

$$D_T = 0.26\frac{k_{bf}}{2k_{bf}+k_p}\frac{\mu_{bf}}{\rho_{bf}}\phi \tag{6b}$$

respectively. Equations (5c) and (5d) are what appear to be the most reliable correlations proposed by Maiga et al. [7], where the subscripts, *p* and *bf* refer to as nanoparticle and base fluid, respectively. Moreover, k_{BO} is the Boltzmann constant and d_p is the nanoparticle diameter, which can be anywhere of the order of 1 to 100 nm. Many including Bianco et al. [8, 9] found that the two-component mixture model is quite adequate for describing the nanofluid heat transfer, as supported by Buongiorno using a magnitudes analysis [3]. The energy equation (3) appears to be identical to that of a pure fluid, except that all properties are functions of ϕ. It should be noted that the nanoparticle continuity equation (4) must be treated simultaneously with Equations (1) to (3) for the other dependent variables, since the thermophysical properties strongly depend on the spatial distribution of ϕ. Most previous researchers neglected the spatial variations of thermophysical properties, Brownian and thermophoretic diffusion coefficients. Such Analytical treatments could result in substantial errors. In this study, all these variations will be considered.

VOLUME AVERAGED EQUATIONS FOR CONVECTION WITHIN A NANOFLUID SATURATED POROUS MEDIUM

A dependent variable φ for the nanofluid is decomposed according to $\varphi = \langle\varphi\rangle^f + \tilde{\varphi}$ where $\langle\varphi\rangle^f$ is the intrinsic average whereas $\tilde{\varphi}$ is the spatial deviation from it. Then, the microscopic equations (1) to (4) together with the heat conduction equation in the solid phase are integrated over the local control volume, exploiting the spatial average relationships. The set of the macroscopic governing equations thus obtained for the nanofluid and solid phases in a nanofluid saturated porous medium with uniform porosity ε may be given as follows:

$$\frac{\partial \rho\langle u_j\rangle}{\partial x_j} = 0 \tag{7}$$

$$-\frac{\partial\langle p\rangle^f}{\partial x_i} = \frac{\mu}{K}\langle u_i\rangle + \rho b\sqrt{\langle u_k\rangle\langle u_k\rangle}\langle u_i\rangle \tag{8}$$

$$c_f\frac{\partial\rho_f\langle u_j\rangle\langle T\rangle^f}{\partial x_j} = \frac{\partial}{\partial x_j}\left(\varepsilon^* k_f\frac{\partial\langle T\rangle^f}{\partial x_j} + \varepsilon k_{dis\,jk}\frac{\partial\langle T\rangle^f}{\partial x_k}\right) - h_v\left(\langle T\rangle^f - \langle T\rangle^s\right) \tag{9}$$

$$\frac{\partial}{\partial x_j}(1-\varepsilon^*)k_s\frac{\partial\langle T\rangle^s}{\partial x_j} - h_v\left(\langle T\rangle^s - \langle T\rangle^f\right) = 0 \tag{10}$$

$$\frac{\partial\langle u_j\rangle\langle\phi\rangle^f}{\partial x_j} = \frac{\partial}{\partial x_j}\left(\varepsilon D_B\frac{\partial\langle\phi\rangle^f}{\partial x_j} + \varepsilon D_{dis\,jk}\frac{\partial\langle\phi\rangle^f}{\partial x_k} + \frac{\varepsilon^* D_T}{\langle T\rangle^f}\frac{\partial\langle T\rangle^f}{\partial x_j}\right) \tag{11}$$

It should be reminded that the local thermal equilibrium between nanoparticles and base fluid is assumed, while the local thermal equilibrium between the nanofluid phase and porous matrix solid phase is discarded such that the intrinsic average temperature of the solid phase $\langle T\rangle^s$ differs from that of the nanofluid phase $\langle T\rangle^f$. In the foregoing volume averaged equations, the Forchheimer extended Darcy law for the internal resistance, the Newton cooling law for interfacial heat transfer with the volumetric interstitial heat transfer coefficient h_v, and the gradient diffusion hypotheses for the thermal dispersion with $k_{dis\,ij}$ and particle dispersion with $D_{dis\,ij}$ are used along with the effective porosity ε^* [10, 11] which accounts for the effect of the tortuosity on the stagnant thermal conductivity k_{stag} such that

$$k_{stag} = \varepsilon^* k_f + (1-\varepsilon^*)k_s \text{ where } \varepsilon^* \cong (2+\varepsilon)/3 \tag{12}$$

The details of the derivation of the volume averaged equations may be found in Sakai et al. [6].

FULLY-DEVELOPED FLOW IN A CHANNEL FILLED WITH A NANOFLUID SATURATED POROUS MEDIUM

Referring to Figure 1, we consider the hydrodynamically and thermally fully developed flow in a channel subject to constant heat flux, filled with a nanofluid saturated porous medium. For this case, the volume average equations (7) to (11) reduce to:

$$-\frac{d\langle p\rangle^f}{dx} = \frac{\mu_f}{K}u_D + \rho b u_D^{\,2} \tag{13}$$

$$\rho c u_D\frac{\partial\langle T\rangle^f}{\partial x} = \frac{\partial}{\partial y}\left(\varepsilon^* k_f + \zeta_k\rho c\sqrt{K}u_D\right)\frac{\partial\langle T\rangle^f}{\partial y} - h_v\left(\langle T\rangle^f - \langle T\rangle^s\right) \tag{14}$$

$$\frac{\partial}{\partial y}\left(1-\varepsilon^*\right)k_s\frac{\partial\langle T\rangle^s}{\partial y}-h_v\left(\langle T\rangle^s-\langle T\rangle^f\right)=0 \tag{15}$$

$$\frac{\partial}{\partial y}\left(\left(\varepsilon D_B+\zeta_D\sqrt{K}u_D\right)\frac{\partial\langle\phi\rangle^f}{\partial y}+\frac{\varepsilon^* D_T}{\langle T\rangle^f}\frac{\partial\langle T\rangle^f}{\partial y}\right)=0 \tag{16}$$

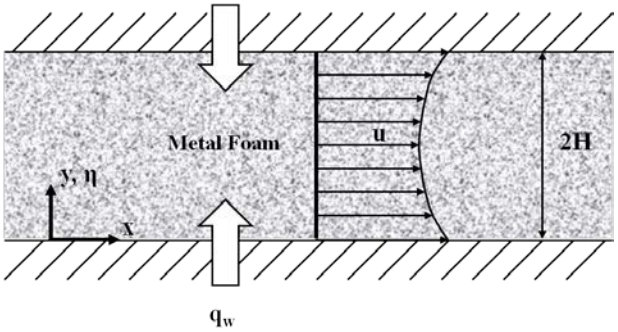

Figure 1: Channel flow subject to constant heat flux

where the streamwise Darcian velocity component of nanofluid is indicated by u_D. The permeability and mechanical dispersion coefficients are given according to the empirical correlations proposed by Calmidi and Mahajan [12, 13] for the case of aluminum foam as follows:

$$K/{d_m}^2=0.00073\left(1-\varepsilon\right)^{-0.224}\left(\frac{1.18}{1-e^{-(1-\varepsilon)/0.04}}\sqrt{\frac{1-\varepsilon}{3\pi}}\right)^{-1.11} \tag{17a}$$

$$bd_m=12\left(1-\varepsilon\right) \tag{17b}$$

$$\varepsilon k_{dis\,yy}=\zeta_k\rho c\sqrt{K}u_D \tag{18a}$$

$$\varepsilon D_{dis_{yy}}=\zeta_D\sqrt{K}u_D \tag{18b}$$

where d_m is the pore diameter. Calmidi and Mahajan [12] suggest $\zeta_k=0.06$, while ζ_D is believed to much smaller than ζ_k. The origin of the vertical coordinate *y* is set on the wall. The boundary conditions are given by

$$q_0=-\left(\varepsilon^* k_f+\zeta_k\rho c\sqrt{K}u_D\right)\frac{\partial\langle T\rangle^f}{\partial y}\bigg|_{y=0}-\left(1-\varepsilon^*\right)k_s\frac{\partial\langle T\rangle^s}{\partial y}\bigg|_{y=0} \tag{19}$$

$$\left(\varepsilon D_B+\zeta_D\sqrt{K}u_D\right)\frac{\partial\langle\phi\rangle^f}{\partial y}\bigg|_{y=0}+\frac{\varepsilon^* D_T}{\langle T\rangle^f}\frac{\partial\langle T\rangle^f}{\partial y}\bigg|_{y=0}=0 \tag{20}$$

$$\frac{\partial\langle\phi\rangle^f}{\partial y}\bigg|_{y=H}=0,\qquad \frac{\partial\langle T\rangle^f}{\partial y}\bigg|_{y=H}=\frac{\partial\langle T\rangle^s}{\partial y}\bigg|_{y=H}=0 \tag{21}$$

Yang et al. [11] considered two extreme cases for the wall temperature difference between the solid and fluid phases, namely, the locally uniform heat flux and locally thermal equilibrium cases, and concluded that the locally thermal equilibrium case is much closer to the reality. Hence, we assume:

$\langle T\rangle^s\big|_{y=0}=\langle T\rangle^f\big|_{y=0}\equiv T_0(x)$: wall temperature

The nanoparticle conservation equation (16) indicates that the diffusion mass flux of the nanoparticles is constant across the channel. Since the wall is impermeable, the boundary condition (20) holds such that the Brownian diffusion flux, mechanical dispersion flux and thermophoretic diffusion flux cancel out everywhere in the channel. The energy equations (14) and (15) may be added and integrated over the lower half the channel from *y*=0 to *H* with the boundary condition (19) and (21) to give

$$\overline{\rho c u_D}\frac{dT_B}{dx}=\frac{q_0}{H} \tag{22}$$

where the subscript 0 refers to the wall at $\eta=0$, and

$$\bar{\varphi}\equiv\frac{1}{A}\int_A\varphi dA=\frac{1}{H}\int_0^H\varphi dy \tag{23}$$

denotes the average over the cross-section such that

$$T_B\equiv\frac{\overline{\rho c u_D\langle T\rangle}}{\overline{\rho c u_D}} \tag{24}$$

is the bulk mean temperature. The foregoing considerations on both nanoparticle diffusion flux and axial temperature gradient are implemented to obtain the analytical expressions in a dimensionless form as follows:

$$u^*(\eta)=\frac{\sqrt{1+4Da^2Hg\dfrac{\left(\rho_f/\rho_{f0}\right)}{\left(\mu_f/\mu_{f0}\right)^2}}-1}{2DaHg\dfrac{\left(\rho_f/\rho_{f0}\right)}{\left(\mu_f/\mu_{f0}\right)}} \tag{25}$$

$$\frac{\rho_f c_f u^*}{\overline{\rho_f c_f u^*}}=-\frac{d}{d\eta}\left(\varepsilon^*\frac{k_f}{k_{stag0}}+\zeta_k Pe\frac{\rho_f c_f}{\rho_{f0}c_{f0}}u^*\right)\frac{dT^{*f}}{d\eta}+Nu_v\left(T^{*f}-T^{*s}\right) \tag{26}$$

$$\left(1-\varepsilon^*\right)\frac{k_s}{k_{stag0}}\frac{d^2T^{*s}}{d\eta^2}-Nu_v\left(T^{*s}-T^{*f}\right)=0 \tag{27}$$

$$\frac{d\langle\phi\rangle^f}{d\eta}=\frac{\varepsilon^*\langle\phi\rangle^f}{N_{BT}\left(1-\gamma T^{*f}\right)\left(\varepsilon\left(1-\gamma T^{*f}\right)+\zeta_D PeLeu^*\right)}\frac{dT^{*f}}{d\eta} \tag{28}$$

The dimensionless coordinate, velocity and temperature are defined as

$$\eta=y/H \tag{29}$$

$$u^*=u_D\Big/\left(\frac{H^2}{\mu_{f0}}\left(-\frac{d\langle p\rangle^f}{dx}\right)\right) \tag{30a}$$

$$T^{*f}=\frac{k_{stag0}\left(T_0-\langle T\rangle^f\right)}{q_0H} \tag{30b}$$

$$T^{*s}=\frac{k_{stag0}\left(T_0-\langle T\rangle^s\right)}{q_0H} \tag{30c}$$

$$N_{BT}\equiv\frac{D_{B0}T_0\phi_0k_{stag0}}{D_{T0}q_0H}=\frac{D_{B0}\phi_0}{D_{T0}\gamma} \tag{31a}$$

$$\gamma\equiv\frac{q_0H}{k_{stag0}T_0} \tag{31b}$$

Furthermore, the Darcy, Lewis, Peclet, Hagen and interstitial Nusselt number s are defined as follows:

$$Da\equiv K/H^2 \tag{32a}$$

$$Le\equiv k_{stag0}/\rho_{f0}c_{f0}D_{B0} \tag{32b}$$

$$Pe\equiv\frac{\rho_{f0}c_{f0}\sqrt{K}}{k_{stag0}}\frac{H^2}{\mu_{f0}}\left(-\frac{d\langle p\rangle^f}{dx}\right) \tag{32c}$$

$$Hg\equiv\frac{\rho_{f0}bH^4}{{\mu_{f0}}^2}\left(-\frac{d\langle p\rangle^f}{dx}\right) \tag{32d}$$

$$Nu_v \equiv \frac{h_v H^2}{k_{stag0}} = 8.72(1-\varepsilon)^{1/4}\left(\frac{1-e^{-(1-\varepsilon)/0.04}}{\varepsilon}\right)^{1/2}\left(\frac{u_D d_m}{\nu}\right)^{1/2} Pr^{0.37}\left(\frac{H}{d_m}\right)^2 \quad (33)$$

Note

$$\rho_{f0} c_{f0} = \phi_0 \rho_p c_p + (1-\phi_0)\rho_{bf} c_{bf} \quad (34a)$$

$$\mu_{f0} = \mu_{bf}\left(1 + 7.3\phi_0 + 123\phi_0^{\,2}\right) \quad (34b)$$

$$k_{stag0} = \left((2+\varepsilon)k_{bf}\left(1 + 2.72\phi_0 + 4.97\phi_0^{\,2}\right) + (1-\varepsilon)k_s\right)/3 \quad (34c)$$

The bulk mean dimensionless temperature is defined as

$$T_B^* = \rho_f c_f u^* T^{*f} / \overline{\rho_f c_f u^*} \quad (35a)$$

Moreover, the thermal properties with the subscript *B* are based on the bulk mean particle volume fraction:

$$\phi_B = u^* \langle \phi \rangle^f / \overline{u^*} \quad (35b)$$

$$u/u_B = u^* / \left(\overline{u^* \rho_f} / \rho_f(\phi_B)\right) \quad (36)$$

The ratio of Brownian and thermophoretic diffusivities ($N_{BT} \propto 1/d_p$) can range over a wide range from 0. 1 to 10 for typical cases of alumina and copper nanoparticles with d_p ~10nm and the bulk mean particle volume fraction ϕ_B ~0.01, while the ratio of wall and fluid temperature difference to absolute temperature $\gamma \sim \left(T_0 - \langle T \rangle_B^f\right)/T_0$ is usually much smaller than unity, as estimated by Buongiorno [3]. In reality, the bulk mean particle volume fraction ϕ_B is prescribed instead of that at the wall ϕ_0. However, for the sake of computational convenience, ϕ_0 is prescribed and ϕ_B is calculated later to find out ϕ_0 as a function of ϕ_B.

Exact solution for the uniform particle distribution in a channel

When the Brownian diffusion overwhelms the thermophoretic diffusion, such that $N_{BT} \to \infty$, the nanoparticles distribute evenly, namely, $\phi(\eta) = \phi_B$ as can be seen from Eq. (28), $d\phi/d\eta = 0$ and $u^*(\eta)$=const. as given by Eq. (25). For this asymptotic case, Equations (26) to (27) are combined, resulting in a third order differential equation with respect to T^{*s} as

$$\frac{d^3 T^{*s}}{d\eta^3} = \xi^2\left(\frac{dT^{*s}}{d\eta} - \frac{1-\eta}{1+\zeta_k Peu^*}\right) \quad (37)$$

which is subject to the following boundary conditions:

$$T^{*s}\big|_{\eta=0} = \left.\frac{d^2 T^{*s}}{d\eta^2}\right|_{\eta=0} = 0 \quad \text{and} \quad \left.\frac{dT^{*s}}{d\eta}\right|_{\eta=1} = 0 \quad (38)$$

The exact solution is given by

$$T^{*s} = \frac{\eta - \frac{1}{2}\eta^2 - \frac{1}{\xi^2}\left(1 - \frac{\cosh(\xi(1-\eta))}{\cosh\xi}\right)}{1+\zeta_k Peu^*} \quad (39)$$

where

$$\xi = \sqrt{\frac{1+\zeta_k Peu^*}{(1-\varepsilon^*)\frac{k_s}{k_{stag0}}\left(\varepsilon^*\frac{k_f}{k_{stag0}} + \zeta_k Peu^*\right)}\, Nu_v} \quad (40)$$

Once T^{*s} is known, T^{*f} is given by Equation (27) as

$$T^{*f} = \frac{\eta - \frac{1}{2}\eta^2 + \frac{1-\varepsilon^*\frac{k_f}{k_{stag0}}}{\left(\varepsilon^*\frac{k_f}{k_{stag0}} + \zeta_k Peu^*\right)\xi^2}\left(1 - \frac{\cosh(\xi(1-\eta))}{\cosh\xi}\right)}{1+\zeta_k Peu^*} \quad (41)$$

The Nusselt number is estimated as

$$Nu_H = \frac{q_0 H}{k_f(\phi_B)(T_0 - T_B)} = \frac{1}{\frac{k_f(\phi_B)}{k_{stag0}} T_B^*} = \frac{1}{\frac{k_f(\phi_B)}{k_{stag0}}\overline{T^{*f}}} \quad (42)$$

$$= \frac{k_{stag0}}{k_f}\frac{1+\zeta_k Peu^*}{\frac{1}{3} + \frac{1-\varepsilon^*\frac{k_f}{k_{stag0}}}{\left(\varepsilon^*\frac{k_f}{k_{stag0}} + \zeta_k Peu^*\right)\xi^2}\left(1 - \frac{\tanh\xi}{\xi}\right)}$$

These results coincide with those obtained for the case of fluid saturated porous media without nanoparticles [10].

Numerical solution for the non-uniform particle distribution

The third order differential equation with respect to T^{*s}, for the general case is given by

$$\frac{d^3 T^{*s}}{d\eta^3} = Nu_v \frac{\left(\frac{k_{stag}}{k_{stag0}} + \zeta_k Pe\frac{\rho_f c_f}{\rho_{f0} c_{f0}} u^*\right)\frac{dT^{*s}}{d\eta} - \int_\eta^1 \frac{\rho_f c_f u^*}{\rho_{f0} c_{f0} u^*} d\eta}{\left(\varepsilon^*\frac{k_f}{k_{stag0}} + \zeta_k Pe\frac{\rho_f c_f}{\rho_{f0} c_{f0}} u^*\right)(1-\varepsilon^*)\frac{k_s}{k_{stag0}}} \quad (43)$$

and

$$\frac{d\phi}{d\eta} = \frac{\varepsilon^* \phi}{N_{BT}\left(1-\gamma T^{*f}\right)\left(\varepsilon\left(1-\gamma T^{*f}\right) + \zeta_D PeLeu^*\right)}\frac{dT^{*f}}{d\eta} \quad (44)$$

where

$$T^{*f} = T^{*s} - \frac{(1-\varepsilon^*)}{Nu_v}\frac{k_s}{k_{stag0}}\frac{d^2 T^{*s}}{d\eta^2} \quad (45)$$

The foregoing set of the differential equations may easily be solved by using a standard integration scheme such as Runge-Kutta-Gill method (e.g. [14]). The corresponding boundary conditions are given by Eq. (38) for T^{*s} and $\langle \phi \rangle^f\big|_{\eta=0} = \phi_0$ for the particle volume fraction $\langle \phi \rangle^f$.

FULLY-DEVELOPED FLOW IN A CIRCULAR TUBE FILLED WITH A NANOFLUID SATURATED POROUS MEDIUM

Hydrodynamically and thermally fully developed flow in a tube subject to constant heat flux may be treated by writing the governing equations in the cylindrical coordinates (*x*, *r*) shown in Figure 2 as

$$\rho c u_D \frac{\partial \langle T \rangle^f}{\partial x} = \frac{1}{r}\frac{\partial}{\partial r} r\left(\varepsilon^* k_f + \zeta_k \rho c \sqrt{K} u_D\right)\frac{\partial \langle T \rangle^f}{\partial r} - h_v\left(\langle T \rangle^f - \langle T \rangle^s\right) \quad (46)$$

$$\frac{1}{r}\frac{\partial}{\partial r} r(1-\varepsilon^*)k_s \frac{\partial \langle T \rangle^s}{\partial r} - h_v\left(\langle T \rangle^s - \langle T \rangle^f\right) = 0 \quad (47)$$

$$\frac{1}{r}\frac{\partial}{\partial r} r\left(\left(\varepsilon D_B + \zeta_D \sqrt{K} u_D\right)\frac{\partial \langle \phi \rangle^f}{\partial r} + \frac{\varepsilon^* D_T}{\langle T \rangle^f}\frac{\partial \langle T \rangle^f}{\partial r}\right) = 0 \quad (48)$$

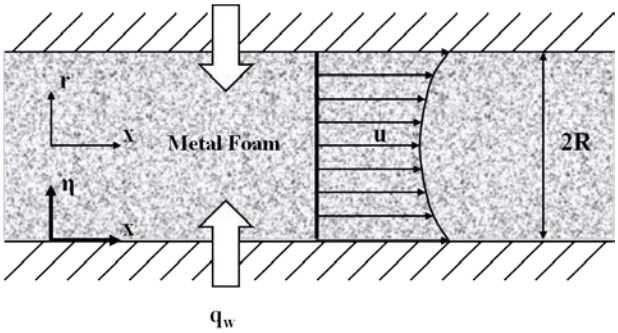

Figure 2: Tube flow subject to constant heat flux

The velocity profile in the tube is the same as that in the channel, as given by Eq. (25). Following the procedure similar to the one used for the channel, the dimensionless set of differential equations for the case of tube filled with a nanofluid-saturated metal foam can readily be obtained as follows:

$$\frac{d^3T^{*s}}{d\eta^3}-\frac{1}{1-\eta}\frac{d^2T^{*s}}{d\eta^2}-\frac{1}{(1-\eta)^2}\frac{dT^{*s}}{d\eta} = Nu_v\frac{\left(\frac{k_{stag}}{k_{stag0}}+\zeta_k Pe\frac{\rho_f c_f}{\rho_{f0}c_{f0}}u^*\right)\frac{dT^{*s}}{d\eta}-\frac{2}{1-\eta}\int_\eta^1\frac{\rho_f c_f u^*}{\rho_{f0}c_{f0}\overline{u^*}}(1-\eta)d\eta}{\left(\varepsilon^*\frac{k_f}{k_{stag0}}+\zeta_k Pe\frac{\rho_f c_f}{\rho_{f0}c_{f0}}u^*\right)(1-\varepsilon^*)\frac{k_s}{k_{stag0}}} \quad (49)$$

and

$$\frac{d\phi}{d\eta}=\frac{\varepsilon^*\phi}{N_{BT}(1-\gamma T^{*f})(\varepsilon(1-\gamma T^{*f})+\zeta_D PeLeu^*)}\frac{dT^{*f}}{d\eta} \quad (50)$$

where

$$T^{*f}=T^{*s}-\frac{(1-\varepsilon^*)}{Nu_v}\frac{k_s}{k_{stag0}}\left(\frac{d^2T^{*s}}{d\eta^2}-\frac{1}{1-\eta}\frac{dT^{*s}}{d\eta}\right) \quad (51)$$

Note that the average value $\overline{\varphi}$ for the case of the tube is computed by

$$\overline{\varphi}\equiv\frac{1}{A}\int_A\varphi dA=\frac{1}{\pi R^2}\int_0^R 2\pi r\varphi dr=2\int_0^1(1-\eta)\varphi d\eta \quad (52)$$

where $\eta=(R-r)/R$. The corresponding dimensionless quantities u^* to Nu_v are defined just as presented in Eqs. (30a) to (33) replacing the channel half height *H* by the radius *R*.

Exact solution for the uniform particle distribution in a tube

For the case of the uniform particle distribution, $N_{BT}\to\infty$, the energy equations (49) and (51) yield the exact solutions as follows:

$$T^{*s}=\frac{\eta-\frac{1}{2}\eta^2-\frac{2}{\xi^2}\left(1-\frac{I_0(\xi(1-\eta))}{I_0(\xi)}\right)}{1+\zeta_k Peu^*} \quad (53)$$

where I_0 is the modified zero order Bessel function of the first kind. The dimensionless fluid temperature is given by

$$T^{*f}=\frac{\eta-\frac{1}{2}\eta^2+\frac{2\left(1-\varepsilon^*\frac{k_f}{k_{stag0}}\right)}{\left(\varepsilon^*\frac{k_f}{k_{stag0}}+\zeta_k Peu^*\right)\xi^2}\left(1-\frac{I_0(\xi(1-\eta))}{I_0(\xi)}\right)}{1+\zeta_k Peu^*} \quad (54)$$

The Nusselt number may be numerically evaluated as

$$Nu_R=\frac{q_0R}{k_f(\phi_B)(T_0-T_B)}=\frac{1}{\frac{k_f(\phi_B)}{k_{stag0}}T_B^*}=\frac{1}{\frac{k_f(\phi_B)}{k_{stag0}}\overline{T^{*f}}} \quad (55)$$

which naturally coincide with the solution reported by Yang et al. [11].

TEMPERATURE DIFFERENCE AND HEAT TRANSFER COEFFICIENT

The effects of Nu_v on the fluid and solid temperature profiles are illustrated in Figure 3. The two temperature profiles overlap each other for sufficiently large Nu_v, in which the local thermal equilibrium holds. In general, the solid temperature is higher than the nanofluid temperature (i.e. T^{*s} is smaller and flatter than T^{*f}).

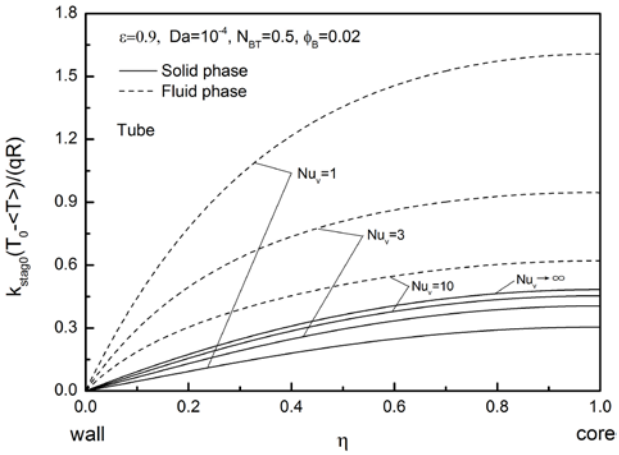

Figure 3: Temperature profiles in a tube

Figure 4 shows the corresponding velocity and particle volume fraction profiles in the tube. The nanoparticle distribution becomes flatter for large Nu_v, since the nanofluid temperature tends to be as uniform as the solid temperature, as witnessed in Figure 3. The velocity is higher near the heated wall where the viscosity is less since the thermophoretic diffusion dominates over the Brownian diffusion, driving the nanoparticles away from the wall.

The heat transfer coefficient ratios $h(\phi_B)/h_{bf}$ with infinite Nu_v are presented against the dimensionless pumping power:

$$P.P.(Hg;Da)\equiv\left(-\frac{d\langle p\rangle^f}{dx}u_B\right)\left(\frac{\rho_0{}^2b^2R^6}{\mu_0{}^3}\right)=\frac{\sqrt{1+4Da^2Hg}-1}{2Da}Hg \quad (56)$$

in a possible range of 6.0×10^9-1.3×10^{15} (corresponding to u_B = 0.01 to 1 m/s, 2*R*=0.02m, *d*m=0.001m) in Figure 5 for the tube. The figure clearly shows that the heat transfer coefficient of a tube filled with a nanofluid saturated metal foam is at least 23 times higher than that of a tube filled with a base fluid. The ratio increases towards 80 to 100 with the pumping power *P.P.* , as the thermal dispersion becomes

significant. Naturally, higher volume fraction of nanofluid results in higher heat transfer coefficient, especially when *P.P.* is large such that the thermal dispersion is dominant. Thus, the combination of the metal foams and nanofluids, results in unconventionally high heat transfer coefficients.

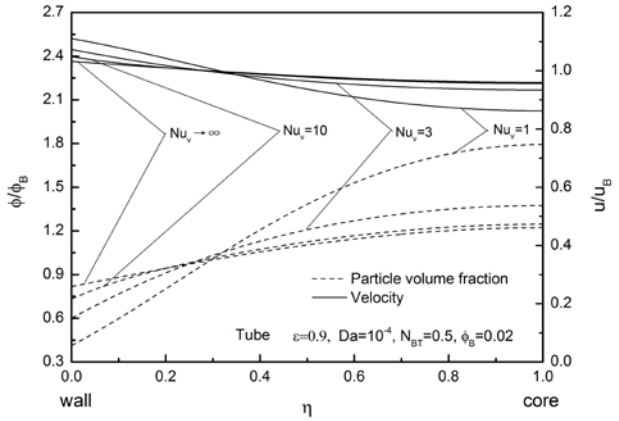

Figure 4: Velocity and nanoparticle volume fraction

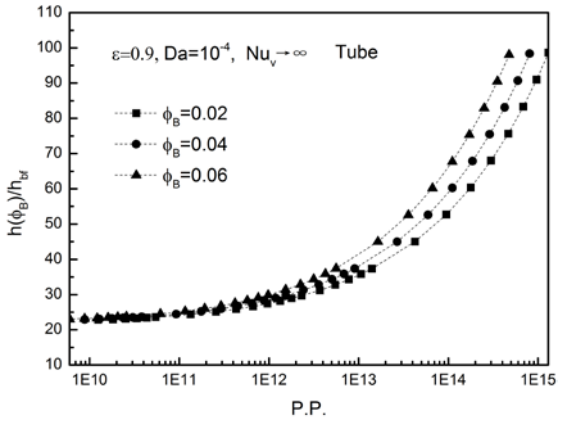

Figure 5: Heat transfer coefficient ratio

CONCLUSIONS

A complete set of the volume averaged governing equations for heat transfer in nanofluid saturated porous media was presented for the first time and solved analytically for the case of uniform particle distribution and numerically for the general case of thermal non-equilibrium. An unconventionally high level of the heat transfer rate (i.e. 80 to 100 times more than the case of base fluid convection without a metal foam) may be achieved by combination of the metal foam and nanofluid.

REFERENCES

[1] Yang, C., Li, W., Sano, Y., Mochizuki, M., Nakayama, A., On the anomalous convective heat transfer enhancement in nanofluids: A theoretical answer to the nanofluids controversy, J. Heat Transfer, 135, 054504, 9 pages, (2013).

[2] Yang, C., Li, W. and Nakayama, A., Convective heat transfer of nanofluids in a concentric annulus, Int. J. Thermal Sci., 71, pp. 249-257, (2013).

[3] Buongiorno, J., Convective transport in nanofluids, J. Heat Transfer, 128, pp. 240-250, (2006).

[4] Maghrebi, M. J., Nazari, M., Armaghani, T., Forced Convection Heat Transfer of Nanofluids in a Porous Channel, Transp Porous Med, 93, pp. 401–413, (2012).

[5] Memari, M., Golmakani, A., Dehkordi, A., "Mixed-Convection Flow of Nanofluids and Regular Fluids in Vertical Porous Media with Viscous Heating," Industrial & Engineering Chemistry Research, 50, pp. 9403–9414, (2011).

[6] Sakai, F., Li, W., Nakayama, A., A rigorous derivation and its applications of volume averaged transport equations for heat transfer in nanofluid saturated metal foams, Int. Heat Transfer Conf. 15, (2014).

[7] Maiga, S. B., Palm, S. J., Nguyen, C. T., Roy, G., Galanis, N., Heat transfer enhancement by using nanofluids in forced convection flows, Int. J. Heat Fluid Flow, 26, pp. 530-546, (2005).

[8] Bianco, V., Manca, O., Nardini, S., Numerical simulation of water/Al2O3 nanofluid turbulent convection, Advances in Mechanical Engineering, 2010, Article ID 976254, pp. 1-10, (2010).

[9] Bianco, V., Chiacchio, F., Manca, O., Nardini, S., Numerical Investigation of Nanofluids Forced Convection in Circular Tubes, Applied Thermal Engineering, 29 (17-18), pp. 3632-3642, (2009).

[10] Kuwahara, F., Yang, C., Ando, K., Nakayama, A., Exact solutions for a thermal nonequilibrium model of fluid saturated porous media based on an effective porosity, J. Heat Transfer, 133, 112602, 9 pages, (2011).

[11] Yang, C., Ando, K., Nakayama, A., A local thermal non-equilibrium analysis of fully developed forced convective flow in a tube filled with a porous medium, Transp Porous Med,89, pp. 237-249, (2011).

[12] Calmidi, V. V., Mahajan, R. L., "The effective thermal conductivity of high porosity fibrous metal foams," J. Heat Transfer, 121, pp. 466-471, (1999).

[13] Calmidi, V. V., Mahajan, R. L., "Forced convection in high porosity metal foams," J. Heat Transfer, 122, pp. 557-565, (2000).

[14] Nakayama, A., PC-Aided Numerical Heat Transfer and Convective Flow, CRC Press, Boca, Raton, pp. 49-50, 103-115, (1995).